Available online at www.sciencedirect.com
SCIENCE DIRECT®
ELSEVIER
International Journal of Impact Engineering 32 (2006) 1384–1402
INTERNATIONAL JOURNAL OF IMPACT ENGINEERING
www.elsevier.com/locate/ijimpeng

The uniaxial stress versus strain response of pig skin and silicone rubber at low and high strain rates

Oliver A. Shergold, Norman A. Fleck*, Darren Radford

Cambridge University Engineering Dept., Trumpington St., Cambridge, CB2 1PZ, UK

Received 22 July 2004; received in revised form 28 November 2004; accepted 30 November 2004
Available online 19 March 2005

Abstract

The uniaxial compressive responses of silicone rubber (B452 and Sil8800) and pig skin have been measured over a wide range of strain rates (0.004–4000 s^{-1}). The uniaxial tensile response of the silicone rubbers was also measured at low strain rates. The high strain rate compression tests were performed using a split-Hopkinson pressure bar made from AZM magnesium alloy. High gain semi-conductor strain gauges were used to detect the low levels of stress (1–10 MPa), and a pulse shaper increased the rise time of dynamic loading on the specimen. The experiments reveal that pig skin strain hardens more rapidly than silicone rubbers and has a greater strain rate sensitivity: pig skin stiffens and strengthens with increasing strain rate over the full range explored, whereas silicone rubber stiffens and strengthens at strain rates in excess of 40 s^{-1}. A one term Ogden strain energy density function adequately describes the measured constitutive response of each solid, and a strategy is outlined for determining the associated material constants (strain hardening exponent and a shear modulus). The strain rate sensitivities of the pig skin and two silicone rubbers are each quantified by an increase in the shear modulus with increasing strain rate, with no attendant change in the strain hardening exponent. It is shown that the Mooney-Rivlin model is unable to describe the strong strain hardening capacity of these rubber-like solids.

Keywords: High strain rate; Hopkinson bar; Rubber; Skin

*Corresponding author.

0734-743X/$ - see front matter © 2005 Elsevier Ltd. All rights reserved.
doi:10.1016/j.ijimpeng.2004.11.010

1. Introduction

The strain rate sensitivity of the stress–strain response of soft solids, such as skin and rubber, is of widespread importance. Applications range from predicting the penetration pressure of skin by a hypodermic needle [1,2] or a high-speed liquid jet [3] in order to administer an injection, to soft tissue damage due to car crashes and stabbing incidents [4]. The strain rate associated with these applications ranges from less than $0.1\,s^{-1}$ to above $1000\,s^{-1}$. There is a pressing need within the pharmaceutical industry to develop in-vitro substitutes for skin in order to develop and test devices for drug delivery [1–3]. Pig skin has a similar mechanical response to that of human skin and is a candidate. But it is preferable to select a synthetic solid for ease of use and repeatability. Silicone rubbers are candidate model materials and in order to compare them with pig skin it is necessary to measure the basic mechanical properties of each. This motivates the choice of materials in the present study.

1.1. Measurement of the constitutive response of soft materials over a wide range of strain rates

Conventional mechanical test machines are used to perform uniaxial tensile and compressive stress versus strain tests at low to medium strain rates (10^{-3}–$10^{1}\,s^{-1}$). At high rates of strain (10^{3}–$10^{4}\,s^{-1}$), a split-Hopkinson pressure bar (SHPB) is an established method for determining the stress versus strain response of a solid in compression [5], tension [6] or torsion [7].

The dynamic testing of strong solids, such as metals and engineering plastics, with a SHPB is common-place (see for example the review by Gray [8]), but soft solids have received much less attention. Limited studies have been conducted on the compressive high strain rate response of various rubbers [9–11], but no data have been found in the literature on the high strain rate testing of soft biological materials, such as skin, using a SHPB. The paucity of data arises from the difficulties of conducting accurate tests on soft solids using the SHPB technique [12]: the stresses are low (on the order of 1–10 MPa) [12], and force equilibrium may not be achieved within the specimen before a significant proportion of the overall test time has elapsed [10].

1.2. Strain rate sensitivity of the constitutive response of skin and rubber

A limited number of studies [13,14] indicate that the constitutive response of skin is sensitive to the magnitude of strain rate within the range 0.1–$10\,s^{-1}$. For example, Haut [13] and Dombi et al. [14] conducted uniaxial tensile tests on rat skin at strain rates of 0.3–$60\,s^{-1}$ and found a 50–100% increase in the ultimate tensile strength with increased strain rate, although the failure strain was unchanged.

Unfortunately, there are no reported data in the literature on the compressive or tensile stress versus strain response of mammalian skin at strain rates above $100\,s^{-1}$. The response of skin to a high frequency oscillation has been investigated, although such experiments are unable to determine the constitutive behaviour of skin due to the combined contribution from the different layers of the skin (see for example Pereira et al. [15] and Potts et al. [16]).

Likewise, the strain rate sensitivity of the uniaxial constitutive response of rubbers has received limited attention [11,17–19]. However, there are few studies for a wide range of strain rates

(10^{-3}–$10^{3}\,s^{-1}$). Gray et al. [20] conducted an extensive characterisation of the uniaxial compression response of Adiprene L-100 rubber over a wide range of strain rate and temperature. They observed little change in constitutive behaviour for strain rates in the range 10^{-3}–$10^{-1}\,s^{-1}$, but the Young's modulus increased by a factor of eight when the strain rate was increased from $10^{-3}\,s^{-1}$ to $3\times10^{3}\,s^{-1}$.

Uniaxial tensile tests [17,18] and compression tests [11,19] on rubbers indicate that the Young's modulus is more sensitive to the strain rate $\dot{\varepsilon}$ within the range $10\,s^{-1}<\dot{\varepsilon}<10^{3}\,s^{-1}$ than within the range $10^{-3}\,s^{-1}<\dot{\varepsilon}<10\,s^{-1}$. For example, Kakavas [17] performed tensile tests on nitrile rubber and found that at an engineering strain of 0.6, the tangent modulus increased by 50%, as the strain rate increased from 5×10^{-4} to $0.1\,s^{-1}$. Jones [18] showed that the tangent modulus of polyurethane (at an unspecified strain measure of 0.48) increased by 250% when the strain rate was increased from 1 to $200\,s^{-1}$. The increase in compressive tangent modulus with increasing strain rate is similar to that observed for the tensile tangent modulus. Bergström and Boyce [19] showed that the compressive tangent modulus of nitrile and chloroprene rubber at a true strain of 0.45 increased by approximately 10% as the strain rate was increased from 2×10^{-4} to $0.1\,s^{-1}$. And Lee et al. [11] studied three unspecified rubbers and demonstrated that an increase in strain rate from 1 to $5000\,s^{-1}$ resulted in a 400% increase in the compressive tangent modulus at an engineering strain of 0.08.

1.3. Review of the relation between the microstructure of rubbers and skin and their macroscopic constitutive response

The relation between microstructure and constitutive response of rubbers is well understood (see for example Ferry [21]), and can be summarised as follows. The visco-elastic nature of amorphous rubbers derives from the mobility of the polymer chain on the atomic scale (rotations between molecular units) and on the macroscopic scale (straightening of the chain between cross-links) [21]. The strain rate sensitivity reflects the timescale required for these polymer chain re-orientations to take place. At low strain rates the polymer chains have sufficient time to re-orientate themselves and the storage modulus of the rubber is low. At high strain rates, the deformation of the polymer chains is restricted to bending and stretching of the chemical bonds, and the storage modulus of the rubber can increase by upto three orders of magnitude. A similar restriction of chain mobility occurs when a rubber is cooled to below its glass transition temperature. Crystallisation of the polymer also restricts chain mobility and consequently the constitutive behaviour of a crystalline rubber is largely insensitive to strain rate.

The relation between the constitutive behaviour of skin and its microstructure is more complex than rubber, due to the various structures found within skin. Skin comprises two main tissue layers: the dermis and the epidermis. In mammalian skins the dermis is typically twenty times thicker than the epidermis [22] and dominates the overall constitutive behaviour. The dermis is composed of a hydrated, gel-like ground substance with elastin fibres and collagen fibres embedded within it. The collagen fibres are the major structural component of the dermis, accounting for 60–80% [23,24] of the dermis dry weight. Consequently, the constitutive behaviour of skin depends upon the structure and density [25,26] of the collagen fibres found within the dermal layer.

Rat tail tendon and human tendon comprise aligned collagen fibres. Uniaxial tensile tests on these tendons [27,28] indicate that collagen fibres can be considered as elastic-plastic, with a Young's modulus on the order of 1 GPa, a yield strain of 10% and a failure strain of 20%. However, the constitutive response of skin cannot be explained solely in terms of the constitutive properties of an individual collagen fibre.

Fig. 1 compares the uniaxial tensile stress versus strain response for human skin [29], pig skin [4] and rat skin [14]. Human skin has a low stiffness (Young's modulus ca. 0.3–1.0 MPa) at low strains, undergoes significant strain hardening at an engineering strain of ca. 0.6 and does not fail until an engineering strain in excess of 1.0 has been achieved. This J-shaped stress versus strain curve is typical for mammalian skin, although the strain hardening characteristic varies from species to species.

The greater compliance of skin, compared to an individual collagen fibre, is attributed to the capacity of the network of fibres to straighten and align in the direction of an applied strain [30,31]. Consequently, at low engineering strains (<0.3) the constitutive response of skin is dominated by the bending stiffness of the collagen fibres and the viscous shear between the fibres and the ground substance [32], whilst at high engineering strains (>0.5) the constitutive response of skin is dominated by the tensile elastic response of the collagen fibres. At high engineering strains (>0.6) this assumption appears to be satisfactory: the tangent modulus of skin of 20–70 MPa [26,29,33] is approximately 3–10% of the Young's modulus of a collagen fibre. This is comparable to the 10% volume fraction of the hydrated collagen within skin [34].

It is well-recognised that the collagen fibres in skin have a preferred orientation, known as Langer lines, due to pre-tension in the skin. The onset of strain hardening begins at lower strains parallel to the direction of pre-tension than transverse to the direction of pre-tension. Consequently, mammalian skin behaves as an orthotropic solid [24,35,36]. This is evidenced by the uniaxial tensile response of pig skin [4] along two orthogonal directions, as shown in Fig. 1.

Collagen fibres (of diameter ca. 5–10 μm [30,37]) comprise bundles of collagen fibrils (of diameter ca. 60 nm [38]) aligned parallel to a hyaluronic acid chain (a long, unbranched,

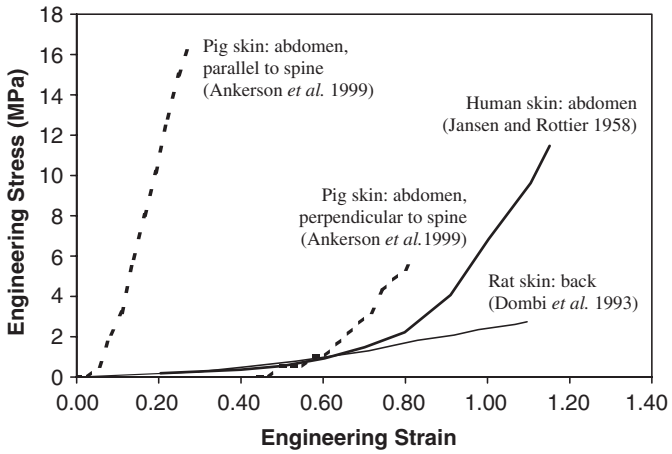

Fig. 1. Tensile uniaxial engineering stress versus engineering strain response for human, pig and rat skin.

polysaccharide found within the ground substance), and linked to the hyaluronic acid by proteoglycan side-chains. Hence, the strain rate sensitivity of the constitutive behaviour of skin is attributed to viscous losses within the ground substance between the collagen fibres [32], and to similar visco-elastic losses within the collagen fibrils [28].

1.4. Constitutive model of skin and silicone rubber

A constitutive model is required to summarise the effect of strain rate upon the measured constitutive response. Constitutive descriptions of solids are based upon either a micromechanical or phenomenological approach. A micromechanical approach is often preferred as these models provide insight into how the micro-structure of the solid affects its constitutive behaviour. Micromechanical models of rubber are based upon the notion that changes of free energy are entropic in nature. In the case of the dermal layer of the skin it is unclear whether the principal source of free energy is entropic or internal energy [39]. The persistence length of collagen fibres is on the order of millimetres while the entanglement length is on the order of microns, and so the origin of stiffness is due to internal strain energy rather than entropy. Some insight into the constitutive behaviour of the dermis is provided by a micromechanical model that considers the alignment and straightening of the fibre network (see for example Refs. [40–42]). However, micromechanical models of fibre networks are inappropriate for describing the constitutive behaviour of rubber.

A phenomenological approach, such as a postulated strain energy density function, is applicable to the description of the constitutive response of both rubber and skin. A number of strain energy density functions have been proposed to describe the constitutive behaviour of skin [39,43] and rubber [44–46]. However, the strain energy density functions that have been proposed to represent the orthotropic behaviour of skin [39] require a large number of constants. Moreover, orthotropic strain energy density functions are not readily available in commercial finite element codes, which are often used in the analysis of non-linear, large deformation problems. Hence, for the purposes of this paper we shall treat skin as an isotropic solid since we shall measure the uniaxial compressive stress versus strain response of skin in the through thickness direction, thereby averaging the response.

The Ogden [44] model for an incompressible, isotropic, hyper-elastic solid is used here to describe the constitutive behaviour of rubber and skin. The Ogden model describes a wide range of strain hardening characteristics and is readily available within finite element codes such as ABAQUS (Hibbit, Karlsson and Sorensen, Pawtucket, Rhodes Island, USA). The one-term Ogden model takes the form

$$\phi = \frac{2\mu}{\alpha^2}(\lambda_1^\alpha + \lambda_2^\alpha + \lambda_3^\alpha - 3), \tag{1}$$

where ϕ is the strain energy density per undeformed unit volume, $(\lambda_1, \lambda_2, \lambda_3)$ are the principal stretch ratios (in a Cartesian reference frame), α is a strain hardening exponent and μ has the interpretation of the shear modulus under infinitesimal straining.

Alternatively, the Mooney-Rivlin model is commonly used to describe rubber-like behaviour. We shall demonstrate that the Mooney-Rivlin model is inappropriate for describing constitutive responses that have a strong strain-hardening characteristic (see also Jerrams et al. [47] and Miller

and Chinzei [48]). The Mooney-Rivlin model takes the form

$$\phi = C_1\left(\lambda_1^2+\lambda_2^2+\lambda_3^2-3\right)+C_2\left(\frac{1}{\lambda_1^2}+\frac{1}{\lambda_2^2}+\frac{1}{\lambda_3^2}-3\right), \tag{2}$$

where C_1 and C_2 are constants. Under infinitesimal straining, where the material response approximates to a linear elastic solid, we have

$$C_1 + C_2 = \tfrac{1}{2}\mu. \tag{3}$$

The necessary and sufficient conditions for ϕ to be positive are given by the inequalities [46]

$$C_1 \geqslant 0, \quad C_2 \geqslant 0. \tag{4}$$

1.5. Outline of the paper

The main objective is to compare the strain rate sensitivity of pig skin and silicon rubbers over a wide range of strain rates (10^{-3}–$10^{3}\,s^{-1}$). We begin by describing a series of compressive uniaxial stress versus strain tests on pig skin and two grades of silicone rubber over a wide range of strain rates. The uniaxial tensile stress versus strain response of the silicone rubbers is also measured. Next, we identify an appropriate constitutive model to describe the measured constitutive response, and outline a strategy for fitting the model to the data. The paper closes with a discussion of the strain rate sensitivity of pig skin and silicone rubbers.

2. Experiments

Uniaxial compression tests were conducted on circular cylindrical specimens of silicone rubber (B452 and Sil8800) and pig skin at strain rates of 4×10^{-3}, 0.4, 40 and $4000\,s^{-1}$. In addition, the tensile uniaxial stress versus strain response of the silicone rubbers was measured at a strain rate of $0.3\,s^{-1}$. Consider first the choice of materials for this investigation.

2.1. Materials

Pig skin samples were obtained from a local slaughter house, Dalehead Foods, Linton, UK. Skin and fat tissue was removed from the rump of the pig immediately after slaughter and the residual pig fat was removed from the skin using a sharp scalpel blade. The pig skin was tested within a few hours of slaughter to minimise degradation of the tissue structure.

Pig skin was investigated to avoid the ethical and immunological issues associated with testing human skin. Fig. 1 demonstrates that, compared to other animal models such as a rat, the constitutive response of pig skin is close to that of human skin. In addition, the thickness of the human and pig dermis are similar: for human skin the dermis thickness ranges from 1 mm on the face to 4 mm on the back [24,49,50]), whilst the dermis of the pig varies from 1 to 6 mm in thickness [51]. In contrast, the dermis of a rat or mouse is typically of thickness 0.6 mm [22].

Two formulations of peroxide cured silicone rubber were studied: B452 (off-white, 52 IRHD) supplied by Dunlop Precision Rubber (Shepshed, Leicestershire) and Sil8800 (Red, 80 IRHD)

supplied by Superior Seals (Three Legged Cross, Dorset). Sil8800 is Superior Seals's trade name for an uncured formulation supplied by Dow Corning with the product code S22062-85-02. Further details on these rubbers are given by Shergold and Fleck [2].

Silicone rubber is considered to be a potential in-vitro model for skin, as the constitutive response and strain rate sensitivity of silicone rubber is close to that of skin [2]. Furthermore, silicone rubber does not strain crystallise, and its crystallisation temperature is well below room temperature. Hence, the constitutive properties and strain rate sensitivity of silicone rubber will be insensitive to small changes in room temperature arising from crystallisation of the polymer chains.

2.2. Uniaxial compression experiments

2.2.1. Sample preparation

Disk-shaped specimens of diameter 7.7 mm and thickness 2.0 mm were cut from silicone rubber sheets of dimensions $2.0 \times 125 \times 200$ mm using a leather die punch mounted onto a hand press. The same punch was used to cut disks from the pig skin samples. Compression of the specimen during the cutting process produced a curved rather than straight edge to the specimen, as sketched in Fig. 2. The thickness and diameter of each rubber specimen was measured using a set of verniers, whilst the thickness and diameter of the pig skin specimens was measured using a travelling microscope.

The skin specimens were typically of diameter 7.0 mm and thickness 2.3 mm. A low specimen aspect ratio was chosen to minimise the time required to reach force equilibrium along the axis of the specimen in the high strain rate compression tests. Previous studies using a SHPB indicate that the constraint on the specimen is negligible for aspect ratios within the range of 0.25–0.5 [10,20,52]. A lubricant (Vaseline by Johnson and Johnson) was applied to the end of the faces of the specimen to reduce the level of friction during the compression tests [53].

2.3. High strain rate compression tests

A sketch of the SHPB used for measuring the compressive uniaxial stress versus strain response of silicone rubber and pig skin, at strain rates of between 1500 and 5000 s^{-1}, is given in Fig. 3a. The SHPB was operated as follows. A striker bar was accelerated along a gun barrel by pressured nitrogen gas (0.05–0.1 MPa). The striker bar velocity (4–10 ms^{-1}) was measured using two light sensors at a spacing of 50 mm. Impact of the striker bar against the end of the input bar caused an

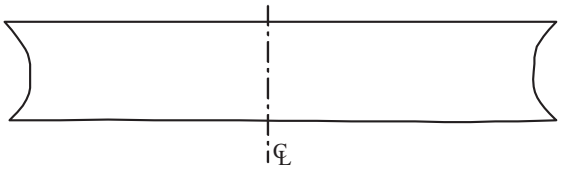

Fig. 2. Sketch of a silicone rubber specimen cut using an 8 mm diameter leather die punch. The punching operation results in a specimen with curved edges, reducing the effective diameter of the specimen.

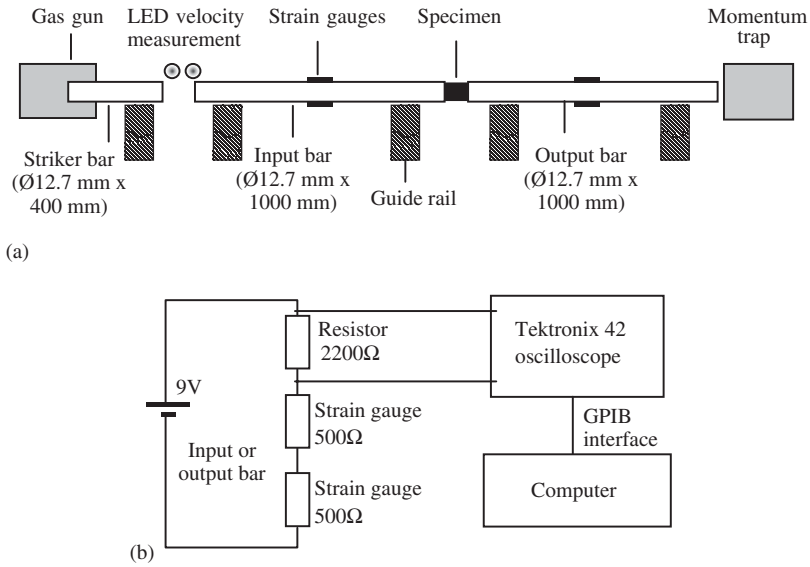

Fig. 3. (a) Sketch of a compressive split-Hopkinson pressure bar used for testing soft materials and (b) sketch of the circuit used for measuring the strain in the pressure bar by recording the change in the voltage across a resistor.

elastic compression wave (incident wave) to propagate along the input bar. The resulting displacement of the input bar compressed the cylindrical specimen sandwiched between the input bar and an output bar. A fraction of the compression wave was transmitted through the specimen and into the output bar, whilst the remainder was reflected back along the input bar as a tensile wave. Strain gauges mounted mid-way along the input and output bars measured the bar strain as the incident, reflected and transmitted waves pass. These strain gauge readings were used to determine the stress versus strain response of the specimen.

The striker bar (of length 0.4 m), input bar (of length 1.0 m) and output bar (of length 1.0 m) were each made from 12.73 mm diameter AZM magnesium alloy rods supplied by Newmet Kock (Waltham Abbey). Magnesium alloy was chosen to maximise the axial strain in the bars, as magnesium alloys have the lowest density (1800 kg m^{-3}) and lowest Young's modulus (44 GPa) of all metallic alloys readily available in rod form [12]. Metallic pressure bars are preferable to polymeric pressure bars as they avoid the complications of dispersion and attenuation of the stress wave as it propagates along the bar [54–56].

A pulse shaper was used to improve the accuracy of the test by increasing the rise time of the leading edge of the incident wave [10,57,58]. Pulse shapers take the form of disks of soft materials such as paper, plastic, or copper mounted on to the striker end of the input bar [8,10,58,59]. The pulse shaper used in the silicone rubber and pig skin compression tests was constructed from two paper disks of diameter 12.5 mm and thickness 0.1 mm, stuck to the striker end of the input bar using Vaseline.

The velocity of the striker was limited to ensure that the magnesium alloy did not yield during the impact between the striker and the input bar. Although the yield strength of the magnesium alloy (80 MPa) theoretically limits the striker impact velocity to 18 m s^{-1}, in practice a safety

margin is allowed for, and the striker was rarely fired at velocities in excess of $10\,\mathrm{m\,s^{-1}}$. Striker velocities of below $4\,\mathrm{m\,s^{-1}}$ could not be reliably produced due to barrel friction.

The axial strain in the input bar and output bar was measured by two semi-conductor strain gauges (AFP-500-090 supplied by Kulite Sensors, Basingstoke) bonded diametrically opposite to each other, and mid-way along the length of each bar. Semi-conductor strain gauges were preferred to conventional foil gauges as they are more sensitive: the AFP-500-090 gauges have gauge factors of 140, whereas foil gauges have gauges factors of about 2. The gauges were bonded onto the bars using a two-part room temperature cure adhesive AE10 (Micro-measurements, Basingstoke).

The two AFP-500-090 gauges were connected in series with a $2200\,\Omega$ resistor, as shown in Fig. 3b. The axial strain was detected by measuring the change in the voltage across the series resistor. A Tektronix TDS420A oscilloscope measured and recorded the voltage versus time response during a compression test. Following the test, the data were downloaded from the oscilloscope to a PC via a GPIB link and stored as a Matlab file for subsequent analysis.

The engineering strain $\varepsilon_s(t)$ in the specimen at time t is given by [8]

$$\varepsilon_s(t) = \frac{c_b \int_0^t [\varepsilon_i(t) - \varepsilon_r(t) - \varepsilon_t(t)]\,\mathrm{d}t}{\ell_s}, \tag{5}$$

where $c_b = 4965\,\mathrm{m\,s^{-1}}$ is the measured value of elastic wave speed in the magnesium bar, $\varepsilon_i(t)$ and $\varepsilon_r(t)$ are the engineering axial strains in the input bar associated with the incident wave and reflected wave, $\varepsilon_t(t)$ is the engineering axial strain in the output bar associated with the transmitted wave and ℓ_s is the undeformed length of the specimen.

The engineering stress $\sigma_s(t)$ in the specimen at time t is calculated from the axial strain in the input bar or output bar at a location adjacent to the specimen [8]

$$\begin{aligned} \sigma_s(t) &= E_b[\varepsilon_i(t) + \varepsilon_r(t)], \\ \sigma_s(t) &= E_b\varepsilon_t(t), \end{aligned} \tag{6}$$

where E_b is the Young's modulus of the input and output bars. The second of these two equations is used to calculate the stress in the specimen.

2.4. Medium strain rate compression tests

Medium strain rate ($40\,\mathrm{s^{-1}}$) uniaxial compression tests were performed using a Schenk Hydropuls PSA 0143 hydraulic testing machine equipped with a PZV 2096 load cell. The cylindrical specimen was placed on the bottom platen of the testing machine and the platen was driven vertically upwards until the specimen just touched the top platen. The displacement at which this initial contact occurred was noted, and the bottom platen was then retracted by 5 mm. This stand-off distance enabled the bottom platen to accelerate to the test speed of $0.8\,\mathrm{m\,s^{-1}}$ before the specimen began to be compressed against the top platen. Towards the end of each test, the platen decelerated to rest: compression data were discarded once the speed had dropped to below $0.7\,\mathrm{m\,s^{-1}}$. Consequently the maximum shortening achievable at the desired strain rate is about $\lambda = 0.4$.

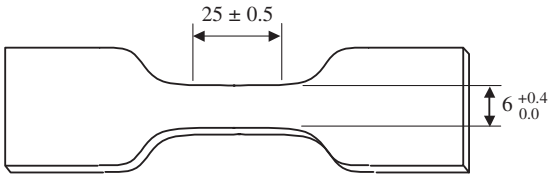

Fig. 4. Dog-bone specimen used for uniaxial tensile tests (dimensions in mm). Thickness = 2 mm.

2.5. Low strain rate compression tests

Low strain rate (0.004 and 0.4 s^{-1}) compression tests were conducted using an Instron 5500R screw driven testing machine. A cylindrical specimen was placed between two platens, with the bottom platen mounted on an Instron 2511-317 load cell. The top platen was driven down until it just touched the top face of the specimen. This marked the start of the test. The top platen was then driven a further 1.3 mm at a speed of either 0.5 mm min^{-1} or 50 mm min^{-1}. The load on the bottom platen, and the displacement of the top platen (via an LVDT), were recorded during each test.

2.6. Uniaxial tensile testing of silicone rubber

The tensile uniaxial stress versus strain response was measured for each silicone rubber at a strain rate of 0.3 s^{-1}. The tests were performed according to the procedure detailed in ISO37 [60] and summarised as follows. Dog-bone test pieces were cut from 2 mm thick silicone rubber sheets, as shown in Fig. 4. Clip gauges, with an initial separation of 25 mm, were attached to the gauge section of the sample to measure the strain. The sample was pulled at a speed of 500 mm min^{-1} using a screw driven testing machine. Three tests were conducted for each grade of silicone rubber and the average response was calculated.

3. Results

The measured compressive and tensile engineering stress versus stretch ratio responses of pig skin and B452 and Sil8800 silicone rubber are shown in Figs. 5–7. The tensile responses of the rubbers were measured to the point of fracture of the specimens. Repeat compressive tests for the pig skin and two rubbers reveal negligible scatter, see Figs. 5–7. The uniaxial tensile stress versus strain response of each silicone rubber is the average response measured from three tests: good repeatability was noted between the tensile tests for each grade of silicone rubber, and a single averaged response is shown. The tensile stress versus strain response of pig skin was not measured, and so we have included the uniaxial tensile test data on pig skin reported by Ankerson et al. [4]. Ankerson et al. [4] removed test samples from the belly of a pig (rather than the rump) and stretched them parallel and perpendicular to the axis of the spine at a strain rate of 0.01 s^{-1}.

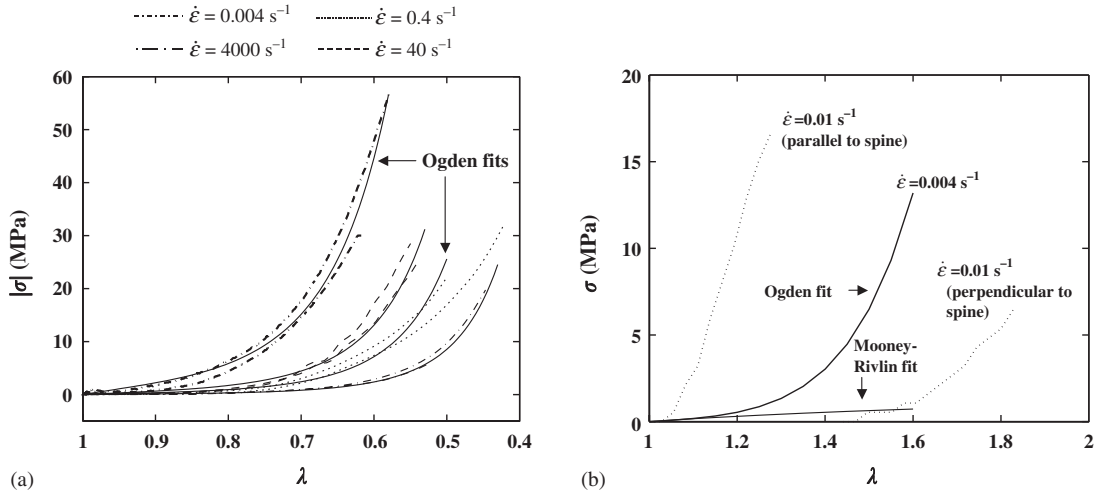

Fig. 5. The engineering stress versus stretch ratio response of pig skin to (a) uniaxial compression and (b) uniaxial tension.

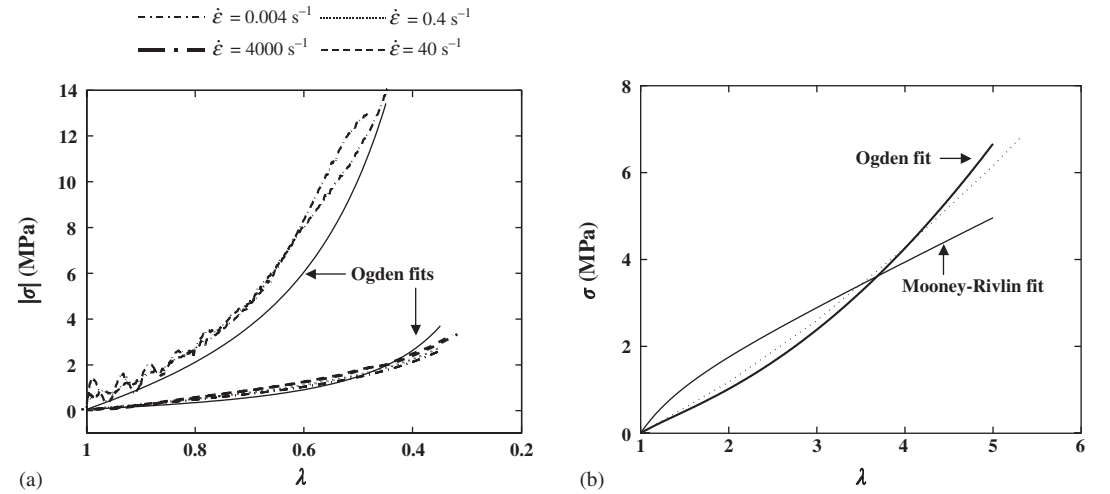

Fig. 6. The engineering stress versus stretch ratio response of B452 silicone rubber to (a) uniaxial compression and (b) uniaxial tension.

The experiments reveal a similar response to an increase in strain rate: there is an increase in the stress level but the shape of the response is unaffected. Qualitatively it can be seen that the two rubbers have a similar shape of stress versus stretch ratio response to that of pig skin. In the high strain rate compression tests, force equilibrium is achieved over the specimen length at a stretch ratio of about 0.95, see Appendix A.

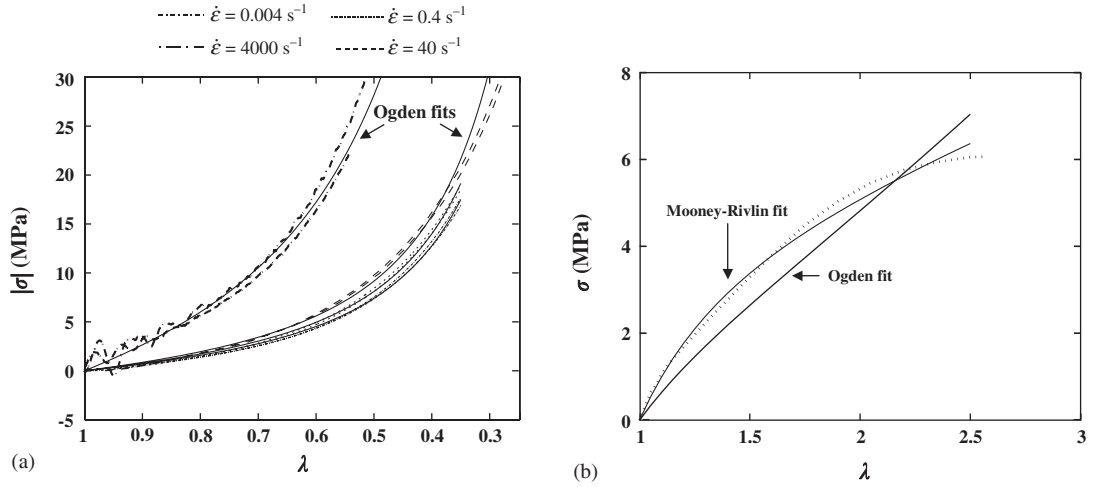

Fig. 7. The engineering stress versus stretch ratio response of Sil8800 silicone rubber to (a) uniaxial compression and (b) uniaxial tension.

4. Discussion

4.1. Evaluating the Ogden constants for a measured constitutive response

The principal nominal engineering stresses σ_{i} $(i = 1, 2, 3)$ are work-conjugate to the principal stretch ratios λ_{i}. Upon assuming the solid is incompressible and characterised by a strain energy density function $\phi(\lambda_i)$, we have

$$\sigma_i = \frac{\mathrm{d}\phi}{\mathrm{d}\lambda_i} - p, \tag{7}$$

where p is a hydrostatic pressure.

The specimen is considered to be in a state of plane stress during a uniaxial compression or tension test. For a Cartesian co-ordinate system, with the z-axis aligned with the loading direction, we can write

$$\sigma_x = \sigma_y = 0 \tag{8}$$

and hence find p in terms of λ_i and σ_z.

The solid is taken as incompressible and so the principal stretch ratios are related by

$$\lambda_x = \lambda_y = \frac{1}{\sqrt{\lambda_z}}. \tag{9}$$

Now specialise to the case of an Ogden strain energy density function (1). This gives

$$\sigma_z = \frac{2\mu}{\alpha}\left[\lambda_z^{\alpha-1} - \lambda_z^{-1-(\alpha/2)}\right]. \tag{10}$$

We seek values for μ and α that minimise the relative least squares error S between the measured and calculated stress during the uniaxial tension or compression test. S is defined by

$$S = \sum_{k=1}^{K} \left(\frac{\sigma_k - \widehat{\sigma}_k}{\sigma_k} \right)^2, \tag{11}$$

where K is the number of data pairs (λ_k, σ_k) in the test data set, λ_k and σ_k are the stretch ratio and engineering stress measured during the test, and $\widehat{\sigma}_k$ is the engineering stress evaluated from (10). A similar strategy is used to evaluate the Mooney-Rivlin constants C_1 and C_2.

4.2. Quality of fit for the Ogden and Mooney-Rivlin models

Figs. 5–7 include the Ogden fits to the measured constitutive response in compression and tension, as well as the Mooney-Rivlin fits to the measured tensile response. The Ogden constants evaluated using (10) and (11) are given in Table 1 for each solid and strain rate considered, whilst the calculated Mooney-Rivlin constants are given in Table 2.

The Ogden model provides a good curve fit for the pig skin and for each grade of silicone rubber at all strain rates considered. The strain hardening exponent α is almost independent of strain rate $\dot{\varepsilon}$ while μ increases monotonically with increasing $\dot{\varepsilon}$. It is argued that the value of α is dictated by the geometric evolution of the collagen network, and is thereby independent of strain rate. In contrast, the resistance to rearrangement by bending of the collagen fibres and by shearing of the intervening ground substance dictate the value of μ, and these deformation mechanisms are sensitive to the strain rate. Note that the Ogden model, evaluated from the pig skin compression

Table 1
Ogden constants [α and μ (MPa)] evaluated at different strain rates for each grade of silicone rubber, pig skin and human skin

Strain rate (s^{-1})	B452 ($\alpha = 3$)	Sil8800 ($\alpha = 2.5$)	Pig skin ($\alpha = 12$)	Human skin ($\alpha = 9$)
0.004	0.4	2.1	0.4	0.11[a]
0.4	0.4	2.3	1.2	
40	0.4	2.6	2.2	
4000	2.8	8.0	7.5	

[a]For this test, $\dot{\varepsilon} = 0.01\,s^{-1}$.

Table 2
Mooney-Rivlin constants evaluated from uniaxial tensile stress versus strain response

	C_1 (MPa)	C_2 (MPa)
Sil8800	1.0	0.9
B452	0.5	0
Human skin	0.3	0

tests at $\dot{\varepsilon} = 0.004\,s^{-1}$, gives a reasonable averaged value for the tensile orthotropic constitutive behaviour of pig skin, as measured by Ankerson et al. [4] at a strain rate of $0.01\,s^{-1}$. Recall that the uniaxial compression tests were performed in the through-thickness direction, and the dermis is almost incompressible [4,24,61]. Thereby, the compression tests give an averaged in-plane tensile response.

A further validation of the accuracy of the Ogden model arises from estimating the Young's modulus E of human skin from the low strain rate shear modulus of human skin ($\mu = 0.11$ MPa). The resulting value of $E = 0.3$ MPa is in reasonable agreement with tensile in vivo measurements of the Young's modulus reported by Clark et al. [62] (0.4–0.8 MPa) and by Manschott and Brakee [63] (0.5 MPa).

The Ogden model accurately describes a wide range of strain hardening behaviours. In comparison, the Mooney-Rivlin model only gives an accurate description of the constitutive behaviour of solids that have a low rate of strain hardening, such as Sil8800. The Mooney-Rivlin function is unable to capture the strain hardening response of solids that have a high rate of strain hardening, such as pig skin. Indeed, even at moderate strain hardening capacities, such as with B452 rubber, the Mooney-Rivlin function does not capture the strain hardening response at high stretch ratios ($\lambda > 4$).

Fig. 8 summarises the relation between the shear modulus and strain rate for the pig skin and silicone rubbers (Sil8800 and B452). In the case of Sil8800 and B452 silicone rubbers, the shear modulus is almost insensitive to strain rate $\dot{\varepsilon}$ for $\dot{\varepsilon} < 40\,s^{-1}$, but increases with increasing strain rate in the high strain rate regime. These results are in accordance with the compressive strain rate sensitivity of rubber reported by Gray et al. [20], Bergström and Boyce [19] and Lee et al. [11].

In contrast, the shear modulus of pig skin increases by a factor of five as the strain rate increases from $\dot{\varepsilon} = 0.004$ to $\dot{\varepsilon} = 40\,s^{-1}$, and by a further factor of four within the range $\dot{\varepsilon} = 40\,s^{-1}$ to $\dot{\varepsilon} = 4000\,s^{-1}$. The increase in stiffness at low rates of strain ($\dot{\varepsilon} = 10^{-4}\,s^{-1}$ to $\dot{\varepsilon} = 10\,s^{-1}$) is in accordance with the measurements on rat skin by Haut [13] and Dombi et al. [14].

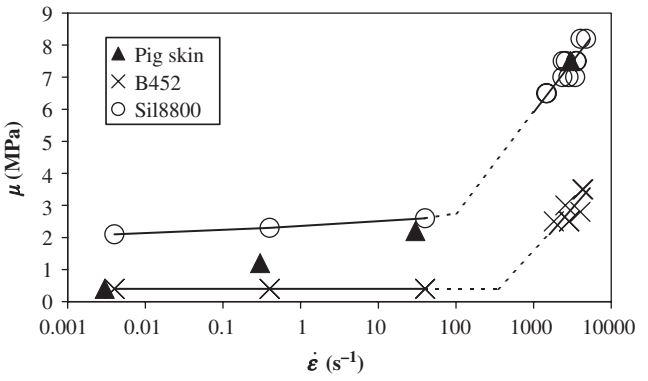

Fig. 8. Shear modulus versus strain rate response of pig skin and B452 and Sil8800 silicone rubber. There are insufficient data with which to construct a curve fitting line for the pig skin.

4.3. Comparison of response of silicone rubber and pig skin

It is noted above that the shear modulus of pig skin increases at a faster rate than the silicone rubbers. Consequently, the selection of a suitable skin substitute will depend upon the strain rate of the application. At a low strain rate the shear modulus of B452 silicone rubber is closer to pig skin than Sil8800 rubber, while at a high strain rate the shear modulus of Sil8800 is similar to that of pig skin. However, silicone rubber may not be an ideal skin substitute as the strain hardening exponent of human skin ($\alpha = 9$) and pig skin ($\alpha = 12$) is considerably greater than that of the silicone rubbers ($\alpha \approx 3$).

5. Concluding remarks

The uniaxial compressive stress versus strain responses of pig skin, and B452 and Sil8800 silicone rubbers, have been measured accurately over a wide range of strain rates. A purpose-built split-Hopkinson pressure bar, constructed from a magnesium alloy and employing semi-conductor strain gauges to detect the bar strain, was able to detect the low sample stress in these soft solids at strain rates within the range 1500–4000 s^{-1}. A pulse shaper was required to minimise the time required for the sample to reach force equilibrium during the high strain rate tests.

The experiments reveal that these soft solids strain harden strongly at high compressive strains. An engineering strain in excess of 0.3 is typically required to capture the shape of the strain hardening response. The constitutive response of pig skin and silicone rubber are also sensitive to the rate of strain. Pig skin stiffens with every decade increase in strain rate, whilst silicone rubber only demonstrates a significantly stiffer response at strain rates in excess of 40 s^{-1}.

The one term Ogden strain energy density function provides a good description of the uniaxial compressive and tensile stress versus strain behaviour of skin and silicone rubber over a wide range of strain rates. This is in contrast to the commonly used Mooney-Rivlin model, which is unable to describe solids with a strong strain hardening characteristic, such as skin and B452 silicone rubber. The one term Ogden model is an attractive choice as it accurately describes the constitutive behaviour of a wide range of strain hardening rates using just two parameters: the strain hardening exponent α and the shear modulus μ. Furthermore, for both grades of silicone rubber and for the pig skin, the strain rate sensitivity is adequately described by an increase in shear modulus with increasing strain rate, with no change in the strain hardening exponent.

Acknowledgements

This research was funded by grants from Weston Medical, the Engineering and Physical Sciences Research Council and the Royal Commission for the Exhibition of 1851.

Appendix A. Force equilibrium in the split-Hopkinson pressure bar tests

The force versus time response for the input bar and output bar are compared to determine the instant during the test when force equilibrium is first achieved. This comparison is shown in Fig. 9

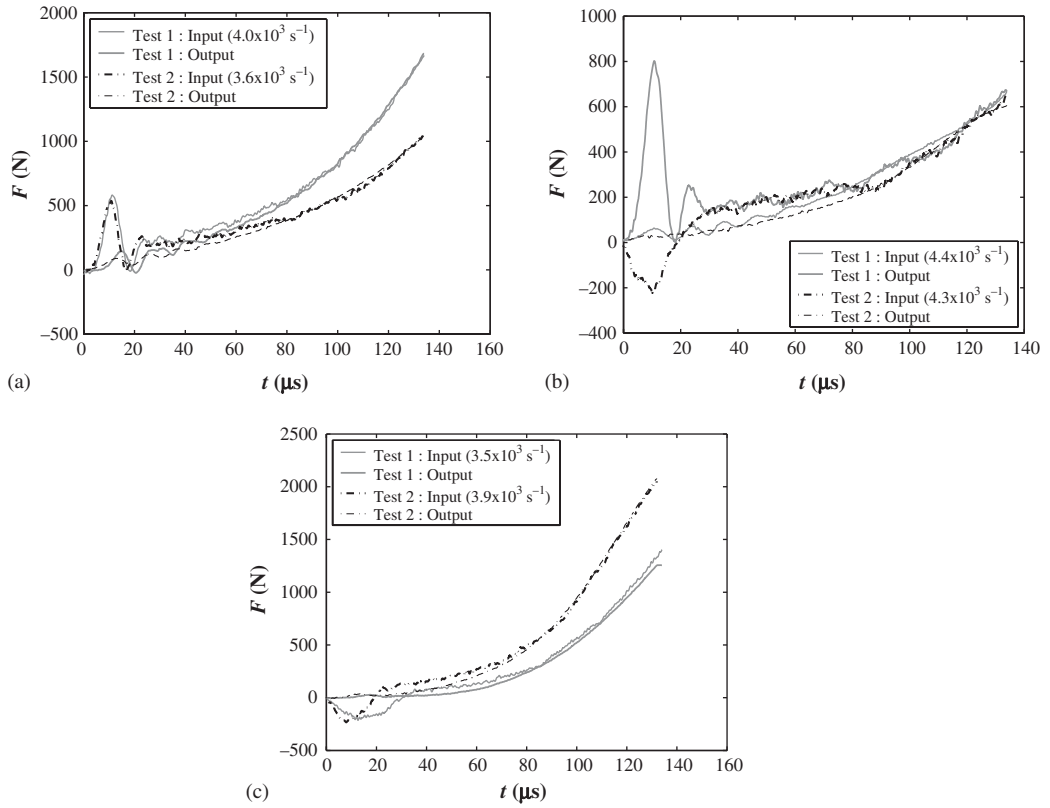

Fig. 9. Compressive force F versus time t response of (a) Sil8800, (b) B452 and (c) pig skin specimens tested at a strain rate of ca. $\dot{\varepsilon} = 4000\,\mathrm{s}^{-1}$.

for split-Hopkinson pressure bar (SHPB) repeat compression tests on pig skin, Sil8800 and B452 silicone rubber specimens at a strain rate of ca. $4000\,\mathrm{s}^{-1}$. In all of the tests, force equilibrium is deemed to have been achieved after 30 μs, equivalent to a compressive stretch ratio of 0.95 for a 2 mm thick specimen being strained at a rate of $4000\,\mathrm{s}^{-1}$.

It is argued that the discrepancy after 30 μs is not due to a violation of equilibrium within the sample. The longitudinal wave speed of rubber is typically on the order of $1000\,\mathrm{m\,s}^{-1}$, and hence the ring-up time for a 2 mm thick specimen (undeformed configuration) should be ca. 6 μs. Also, the inertia of the specimen should be negligible after the first 22 μs of the test [64]. The minor differences that exist between the input bar and output bar measurements after 30 μs are attributed to inaccuracies in the data acquisition system and the method used to interpret the data. The input bar force is calculated as the difference between the incident and reflected waves. At low strains this difference is small in comparison to the overall signal strength. Consequently, at low forces, the input bar force measurement is sensitive to the resolution and calibration of the measurement system, as well as the method used to align the incident and reflected waves. Hence, the output bar measurement of the force on the sample is more accurate than the input bar measurement.

References

[1] Shergold O, Fleck NA. Mechanisms of deep penetration of soft solids, with application to the injection and wounding of skin. Proc R Soc London Ser A 2004;460:3037–58.

[2] Shergold O, Fleck NA. Experimental investigation into the deep penetration of soft solids by sharp and blunt punches, with application to the piercing of skin. ASME J Biomech Eng 2005; to appear.

[3] Shergold O, Fleck NA. The penetration of a soft solid by a liquid jet, with application to the administration of a needle-free injection. J Biomech 2005; submitted.

[4] Ankerson J. Puncture resistance and tensile strength of skin simulants. Proc Inst Mech Eng 1999; 213(Part H):493–501.

[5] Kolsky H. An investigation of the mechanical properties of materials at very high rates of loading. Proc Phys Soc (London) 1949;62B:676–700.

[6] Harding J, Wood EO, Campbell JD. Tensile testing of materials at impact rates of strain. J Mech Eng Sci 1960;2:88–96.

[7] Duffy J, Campbell JD, Hawley RH. On the use of a torsional split Hopkinson Bar to study rate effects in 1100-O aluminium. J Appl Mech (Trans ASME) 1971;38:83–91.

[8] Gray III GT. Classic split-Hopkinson Pressure Bar testing. In: Kuhn H, Medlin D, editors. ASM handbook. Mechanical testing and evaluation, vol. 8. ASM International; 2000. p. 462–74.

[9] Gray III GT, et al. High- and low-strain rate compression properties of several energetic material composites as a function of strain rate and temperature. In: 11th Detontation Symposium. Snow Mass, CO: Amperstand Publishing; 2000.

[10] Chen W, et al. Dynamic compression testing of soft materials. J Appl Mech—Trans ASME 2002;69(3): 214–23.

[11] Lee OS, et al. Dynamic deformation behavior of rubber under high strain rate compressive loading. Int J Mod Phys B 2003;17(8–9):1415–20.

[12] Gray III GT. Split-Hopkinson Pressure Bar testing of soft materials. In: Kuhn H, Medlin D, editors. ASM handbook. Mechanical testing and evaluation, Vol. 8. ASM International; 2000. p. 462–74.

[13] Haut RC. The effects of orientation and location on the strength of dorsal rat skin in high and low speed tensile failure experiments. J Biomech Eng—Trans ASME 1989;111:136–40.

[14] Dombi GW, Haut RC, Sullivan WG. Correlation of high-speed tensile strength with collagen content in control and lathyritic rat skin. J Surg Res 1993;54(1):21–8.

[15] Pereira JM, Mansour JM, Davis BR. The effects of layer properties on shear disturbance propagation in skin. J Biomech Eng—Trans ASME 1991;113:30–5.

[16] Potts RO, Chrisman DA, Buras EM. The dynamic mechanical-properties of human-skin in-vivo. J Biomech 1983;16(6):365–72.

[17] Kakavas PA. Mechanical properties of bonded elastomer discs subjected to triaxial stress. J Appl Polym Sci 1996;59(2):251–61.

[18] Jones JW. Tensile testing of elastomers at ultra-high strain rates. J Appl Polym Sci 1960;IV(12):284–90.

[19] Bergström JS, Boyce MC. Constitutive modeling of the large strain time-dependent behavior of elastomers. J Mech Phys Solids 1998;46(5):931–54.

[20] Gray III GT, et al. Influence of temperature and strain rate on the mechanical behaviour of Adiprene L-100. In: C3 EURODYMAT 97, 1997.

[21] Ferry JD. Viscoelastic properties of polymers, 2nd ed. New York: Wiley; 1970.

[22] Shergold O. The Mechanics of Needle-free Injection. In: Department of Mechanical Engineering. Cambridge University: Cambridge; 2004. p. 200.

[23] Dombi GW, Haut RC. The tensile strength of skin and correlations with collagen content. In: Advances in Bioengineering; ASME: New York, 1985. p. 95–6.

[24] Reihsner R, Balogh B, Menzel EJ. Two-dimensional elastic properties of human skin in terms of an incremental model at the in vivo configuration. Med Eng Phys 1995;17(4):304–13.

[25] Nimni ME, De Guia E, Bavetta LA. Collagen, hexosamine and tensile strength of rabbit skin during ageing. J Invest Dermatol 1966;47(2):156–8.

[26] Vogel HG. Age dependence of mechanical and biochemical properties of human skin. Part I. Stress–strain experiments, skin thickness and biochemical analysis. Bioeng Skin 1987;3:67–91.
[27] Sanjeevi R, Somanathan N, Ramaswamy D. A viscoelastic model for collagen fibres. J Biomech 1982;15(3):181–3.
[28] Haut RC. Age-dependent influence of strain rate on the tensile failure of rat-tail tendon. J Biomech Eng—Trans ASME 1983;105:296–9.
[29] Jansen LH, Rottier PB. Some mechanical properties of human abdominal skin measured on excised strips: a study of their dependence on age and how they are influenced by the presence of striae. Dermatologica 1958;117:65–183.
[30] Millington PF, Wilkinson R. Skin: biological structure and function, 1st ed. Cambridge: Cambridge University Press; 1983.
[31] Finlay B. Scanning electron microscopy of the human dermis under uni-axial strain. Bio-med Eng 1969;4:322–7.
[32] Cohen RE, Hooley CJ, McCrum NG. Viscoelastic creep of collagenous tissue. J Biomech 1976;9:175–84.
[33] Agache PG, et al. Mechanical-properties and Youngs Modulus of human-skin in vivo. Arch Dermatol Res 1980;269(3):221–32.
[34] Tregear RT. Physical functions of skin. In: Danielli JF, editor. Theoretical and experimental biology, Vol. 5. London: Academic Press; 1966. p. 84–8.
[35] Flynn DM, et al. A finite element based method to determine the properties of planar soft tissue. J Biomech Eng 1998;120:202–10.
[36] Lanir Y, Fung YC. Two-dimensional mechanical properties of Rabbit skin—II. Experimental results. J Biomech 1974;7:171–82.
[37] Gartner LP, Hiatt JL. Colour textbook of histology, 2nd ed. Philadelphia, Pennsylvania: W.B. Saunders Company; 2001. p. 19106.
[38] Barton SP, Marks R. Measurement of collagen-fibre diameter in human skin. J Cutaneous Pathol 1984;11: 18–26.
[39] Fung YC. Biomechanics: mechanical properties of living tissues, 1st ed. New York: Springer; 1981.
[40] Lanir Y. Constitutive equations for fibrous connective tissues. J Biomech 1983;16:1–12.
[41] Markenscoff X, Yannas IV. On the stress–strain relation for skin. J Biomech 1979;12:127–9.
[42] Belkoff SM, Haut RC. A structural model used to evaluate the changing microstructure of maturing rat skin. J Biomech 1991;24(8):711–20.
[43] Tong P, Fung YC. The stress–strain relationship for the skin. J Biomech 1976;9:649–57.
[44] Ogden RW. Large deformation isotropic elasticity—on the correlation of theory and experiment for incompressible rubberlike solids. Proc R Soc Lond 1972;A326:565–84.
[45] Ward A. Mechanical properties of solid polymers, 2nd ed. Bristol BS3 2NT: Wiley, J.W. Arrowsmith Ltd.; 1983. p. 44.
[46] Lurie AI. Non linear theory of elasticity. In: Achenbach JD, et al., editors. Applied mathematics and mechanics. New York: Elsevier Science; 1990.
[47] Jerrams SJ, Kaya M, Soon KF. The effects of strain rate and hardness on the material constants of nitrile rubbers. Mater Design 1998;19(4):157–67.
[48] Miller K, Chinzei K. Mechanical properties of brain tissue in tension. J Biomech 2002;35:483–90.
[49] Tan CY, et al. Skin thickness measurement by pulsed ultrasound—its reproducibility, validation and variability. Br J Dermatol 1982;106(6):657–67.
[50] Serup J, et al. High-frequency ultrasound examination of skin: introduction and guide. In: Serup J, editor. Handbook of non-invasive methods and the skin. CRC Press: Boca Raton; 1995. p. 239–56.
[51] Bacha WJJ, Bacha LM. Colour atlas of veterinary histology, 2nd ed. Lippincott Williams & Wilkins; 2000.
[52] Rodriguez J, et al. Numerical study of the specimen size effect in the split Hopkinson Pressure Bar tests. J Mater Sci 1995;30(18):4720–5.
[53] Walley SM, et al. A study of the rapid deformation behaviour of various polymers. Philos Trans R Soc (London) A 1989;A328:1–33.
[54] Zhao H, Gary G. A new method for the separation of waves. Application to the SHPB technique for an unlimited duration of measurement. J Mech Phys Solids 1997;45(7):1185–202.
[55] Bacon C. Separation of waves propagating in an elastic or viscoelastic Hopkinson Pressure Bar with three-dimensional effects. Int J Impact Eng 1999;22(1):55–69.

[56] Bussac MN, et al. An optimisation method for separating and rebuilding one- dimensional dispersive waves from multi-point measurements. Application to elastic or viscoelastic bars. J Mech Phys Solids 2002;50(2):321–49.
[57] Parry DJ, et al. Stress equilibrium effects within Hopkinson bar specimens. J Phys IV 1994;4:C8-107–12.
[58] Frew DJ, Forrestal MJ, Chen W. Pulse-shaping techniques for testing brittle materials with a Split Hopkinson Pressure Bar. Exp. Mech. 2002;42:93–106.
[59] Nermat-Nasser S, Isaacs JB, Starrett JE. Hopkinson techniques for dynamic recovery experiments. Proc Roy Soc London Ser A 1991;A453:371–91.
[60] Bsi. BS903 Physical testing of rubber. Part A2. Method for determination of tensile stress–strain properties, 1995.
[61] North J, Gibson F. Volume compressibility of human abdominal skin. J Biomech 1978;11:203–7.
[62] Clark JA, Cheng JCY, Leung KS. Mechanical properties of normal skin and hypertrophic scars. Burns 1996;22(6):443–6.
[63] Manschot JFM, Brakkee AJM. Characterisation of in vivo mechanical skin properties independent of measuring configuration. Bioeng Skin 1987;3:1–10.
[64] Gorham DA. Specimen inertia in high strain-rate compression. J Phys D: Appl Phys 1989;22:1888–93.